

## Semi-modular Rectangular Broad-crested Flow Meter with Lateral Contraction

Bachir ACHOUR\*

Research Laboratory in Subterranean and Surface Hydraulics (Larhyss)  
University of Biskra, PO Box 145 RP 07000 Biskra Algeria

\* Corresponding author. Tel.: 0021369851544  
E-mail address: bachir.achour@larhyss.net

---

### Abstract

#### Keywords:

*Semi modular flow meter,  
discharge coefficient,  
discharge,  
rectangular contraction,  
weir.*

A particular study of a semi-modular rectangular flow meter, characterized by both a broad-crested sill and lateral contraction, is presented. This is firstly theoretically examined and secondly experimentally tested under various geometrical dimensions. The theoretical development aims, on one hand, to identify the main characteristics of the flow and the geometrical parameters of the flow meter which influence the discharge. On the other hand, discharge coefficient is expressed with the help of the momentum equation applied between two sections judiciously chosen.

Under various geometrical dimensions, the considered flow meter is intensively tested in order to corroborate or to correct the proposed theoretical relationships.

Accepted: 23 August 2013 © Academic Research Online Publisher. All rights reserved.

---

### 1. Introduction

Discharge measurement flowing through a conduit or a channel is one of the oldest problems encountered in engineering practice. Nowadays, this problem is solved differently depending on the type of the chosen flow meter. In the field of free surface flow, overspill structures are preferably used to estimate the amount of runoff. The sharp-crested V-notched weir known as Thomson weir [1, 2, 3, 4] is recommended for its high accuracy especially when it comes to measuring low flow rates. Weirs of the same type but with a rectangular notch [5, 6, 7] are also widely used. However, they are extremely unreliable in estimating low flow rates unlike the Thomson weir. In practice, the so-called hydraulic jump gauges are sometimes used to measure the flow rate. With the exception of Achour's hydraulic jump gauge [8] whose cross section shape is triangular, hydraulic jump gauges are often a rectangular shape. The best known of these are the Venturi and Parshall [1] or the modified Venturi [9]. These devices have the ability to not only measure the flow rate but also to raise the level of

downstream head line which is a real advantage in low slope areas [8]. The flow measuring devices can also be constituted by a broad-crested sill with a triangular notch [10, 11] or rectangular notch [12, 13] with or without height of weir. Their longitudinal profile may take a triangular form or a planar shape. They may also be characterized by a lateral contraction or a local narrowing of their cross section. All these described devices are qualified as semi-modular devices due to the fact that the flow therein depends on both the head over the weir and the geometrical characteristics of these devices. Their peculiarity is to generate a subcritical upstream flow and a supercritical downstream flow inside the weir. The cross section is then the seat of a critical flow and this, from a theoretical point of view, is what allows expressing the discharge which depends on both the upstream flow depth over the weir and the geometrical characteristics of the device [14]. Recently, new developments have been presented regarding the weir circular thin-walled under partially submerged conditions. A new method was suggested for modelling the device as well as the discharge [15, 16].

In this study, a rectangular semi modular broad-crested flow meter with a lateral contraction is theoretically examined and subjected to intense laboratory experiments. The theoretical development aims to establish the discharge coefficient relationship and therefore the discharge, ignoring at first the effect of the approach velocity and taking into account this effect the second time. Parameters influencing the discharge are clearly identified and then transformed into dimensionless terms in order to give them a general validity. In various geometric dimensions, the device is experimentally tested in order to verify the proposed theoretical relationships.

## 2. Description of the Device

Figure 1 is a perspective schematic representation of the considered semi modular flow meter. It is a rectangular cross section broad-crested weir of width  $b$ , extending over a length  $L$ . As with most conventional weirs, the flow meter is characterized by a height  $P$  thereby causing a vertical contraction of the flow. In addition, the apparatus is inserted in a rectangular channel of height  $h_o$  and of width  $B > b$  thereby generating a lateral contraction of the flow. In Figure 1, the flow is from right to left and is characterized by the head  $h_d$  over the weir. It is the upstream flow depth counted over the crest height  $P$ . The slope of the rectangular channel is neglected. Considering both shape of the device and the rectangular channel, the parameters  $L, P, h_d, b$  and  $B$  play a fundamental role in the functioning of the device. The effect of the length  $L$  has not been studied in this research. However, the length  $L$  should be sufficient to allow the occurrence of a critical flow inside the notch of width  $b$ .

Considering the parameters  $P, h_d, b$  and  $B$ , it is possible to form the following dimensionless variable

$P^* = P/h_d$  that represents the relative height of the weir and  $S = b/B$  that reflects the degree or the

ratio of the lateral contraction. In addition,  $P^*$  and  $S$  can form the dimensionless parameter  $\mathcal{E} = S / (1 + P^*)$ . The physical meaning of  $\mathcal{E}$  becomes clear when writing what follows:

$$\mathcal{E} = \frac{b/B}{1 + \frac{P}{h_d}} = \frac{bh_d}{B(P + h_d)} = \frac{\text{contacted section}}{\text{full section}} \quad (1)$$

Thus,  $\mathcal{E}$  represents the ratio of the contracted upstream flow section which varies in the range  $0 < \mathcal{E} < 1$ .

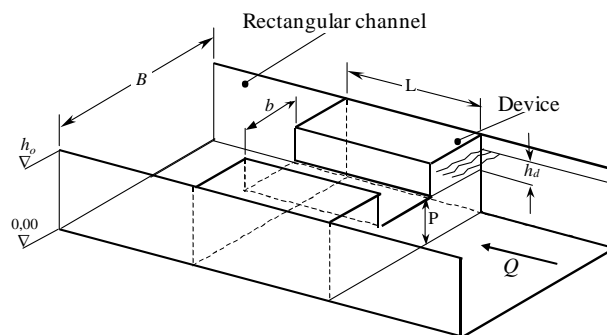


Fig.1. Perspective schematic representation of the device

### 3. Description of the Flow

Figure 2 is a schematic representation of the longitudinal profile of the flow. It is characterized by the subcritical upstream inflow depth  $h_1$  in the section 1-1, the total head  $H_1$ , the upstream approach velocity head  $V^2 / 2g$  and the flow depth  $h_d$  over the weir of height  $P$ .

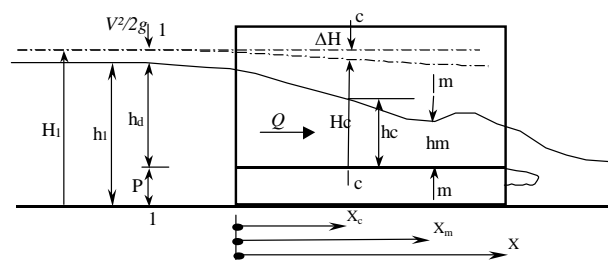


Fig. 2. Longitudinal profile of the flow

Inside the flow meter, the flow undergoes a lowering of the free surface to the section m-m beyond which an elevation of the surface is perceptible. Section m-m is then characterized by a minimum depth denoted  $h_m$  located at the distance  $X_m$  from the inlet of the device. When the length  $L$  of the device is not sufficient, the section of minimum depth cannot be observed. In figure 2,  $\Delta H$  is the head

loss due to the lateral and vertical contractions of the section. From a theoretical point of view,  $\Delta H$  is difficult to estimate with the current state of knowledge. Inside the flow meter, the flow remains subcritical until reaching the control section c-c where the depth  $h_c$  is critical, located at the distance  $X_c$  from the inlet of the device. The critical depth is governed by the following well-known relationship:

$$h_c = \sqrt[3]{\frac{Q^2}{gb^2}} \quad (2)$$

where  $Q$  is the discharge and  $g$  is the acceleration due to gravity. In order to take into account the effect of the approach velocity, it is recommended to consider velocity head  $V^2 / 2g$  as a fraction of the head  $h_d$ . Thus, one may write:

$$V^2 / 2g = u \times h_d \quad (3)$$

The total head  $H_d$  counted over the height weir  $P$  can be then written as:

$$H_d = h_d + \frac{V^2}{2g} = (1+u)h_d \quad (4)$$

It is obvious that  $u$  is less than unity. For  $u \rightarrow 0$ , the approach velocity is negligible and the total head  $H_d$  can be assimilated to the head  $h_d$ . Thus, one can write  $0 \leq u < 1$ .

## 4. Theory

### 4.1. Momentum equation

Application of the momentum theorem in the longitudinal direction yields:

$$\dots Q(V_c - V_1) = F_1 - F_c - F_x \quad (5)$$

in which pressure distribution at the two considered cross sections "1" (upstream) and "c" (downstream) is assumed hydrostatic and corresponding velocity distributions uniform. Note that  $F_x$  denotes the pressure force exerted by the upstream face of the device in channel axis direction  $X$ . In equation (5),  $V_c$  is the mean velocity at the critical cross section c-c,  $V_1$  is the mean velocity at the upstream cross section 1-1 and  $\dots$  is the water density. The pressure forces  $F_1$  and  $F_c$  can be respectively written as  $F_1 = (1/2)\dots gBh_1^2$  and  $F_c = (1/2)\dots gbh_c^2$ , whereas  $F_x$  is governed by  $F_x = \dots g\bar{h}_x A_x$  in which  $\bar{h}_x$  is the depth at the centre of gravity of the cross section area  $A_x$  counted from the free surface flow. It is easy to demonstrate that  $\bar{h}_x = (1/2)(h_1^2 B - h_d^2 b) / A_x$  where  $A_x = (h_1 B - h_d b)$ . Equation (5) may be written as:

$$h_d^{*3} - 3h_d^* + \frac{2S}{1+P^*} = 0 \quad (6)$$

in which  $h_d^* = h_d / h_c$ . The parameters  $S$  and  $P^*$  have already been defined. Inserting equation (1) into equation (6) leads to:

$$h_d^{*3} - 3h_d^* + 2E = 0 \quad (7)$$

Equation (7) shows that the non-dimensional parameter  $E$  is related to the relative head  $h_d^*$  by a cubic equation. The discriminant of equation (7) is  $D = (E^2 - 1)$  which is negative since  $0 < E < 1$ . The real root of equation (7) is then:

$$h_d^* = 2 \cos(r/3) \quad (8)$$

in which:

$$r = \cos^{-1}(-E) \quad (9)$$

Equations (1), (8) and (9) allow a direct computation of the relative head  $h_d^*$  for the known values of the parameters  $b$ ,  $B$ ,  $P$  and  $h_d$ .

#### 4.2. Discharge for a negligible approach velocity

Let us assume  $\sim_o$  as the discharge coefficient for a negligible approach velocity. The discharge  $Q$  is then governed by the following equation valid for a rectangular cross section:

$$Q = \sim_o b \sqrt{2g} h_d^{3/2} \quad (10)$$

Eliminating  $Q$  between equations (2) and (10), one may write:

$$\sim_o = \frac{\sqrt{2}}{2} h_d^{*-3/2} \quad (11)$$

Thus, the discharge coefficient  $\sim_o$  depends solely on the relative head  $h_d^*$  and then on the non-dimensional parameter  $E (S, P^*)$ . Inserting equation (8) in equation (11) yields:

$$\sim_o = \frac{1}{4} \cos^{-3/2}(r/3) \quad (12)$$

Eliminating  $\sim_o$  between equations (10) and (12) leads to:

$$Q = \frac{1}{4} \sqrt{2g} b \left[ \cos^{-3/2}(r/3) \right] h_d^{3/2} \quad (13)$$

Equation (13) expresses the discharge  $Q$  for a negligible approach velocity, bearing in mind that the angle  $r$  is given by equation (9) for the known value of the non-dimensional parameter  $E$ .

### 4.3. Example 1

Compute the discharge  $Q$  flowing in the rectangular channel represented in figure 1 for:

$$B = 1m, b = 0,5m, P = 0,4m, h_d = 0,6m.$$

- i. Let us assume a negligible approach velocity. According to equation (1), the non-dimensional parameter  $\xi$  is then:

$$\xi = \frac{b/B}{1 + P/h_d} = \frac{0.5/1}{1 + 0.4/0.6} = 0.3$$

- ii. Applying equation (9) leads to:

$$r = \cos^{-1}(-\xi) = \cos^{-1}(-0.3) = 1.87548898 \text{ radian}$$

- iii. Applying equation (13), the requested discharge  $Q$  is then:

$$\begin{aligned} Q &= \frac{1}{4} \sqrt{2g} b \left[ \cos^{-3/2}(r/3) \right] h_d^{3/2} \\ &= \frac{1}{4} \times \sqrt{2 \times 9.81} \times 0.5 \times \left[ \cos^{-3/2}(1.87548898/3) \right] \times 0.6^{3/2} = 0.3524 m^3 s^{-1} \end{aligned}$$

### 4.4. Discharge for a significant approach velocity

When the approach velocity of the flow in the inlet channel cannot be neglected, equation (10) shall be reasonably written in the following form:

$$Q = \sim_o b \sqrt{2g} H_d^{3/2} \tag{14}$$

Eliminating the total head  $H_d$  between equations (4) and (14), one may write:

$$Q = \sim_o b \sqrt{2g} (1+u)^{3/2} h_d^{3/2} \tag{15}$$

For  $u \rightarrow 0$  corresponding to a negligible approach velocity, equation (10) is then reproduced.

Equation (15) can be rewritten as:

$$Q = \sim b \sqrt{2g} h_d^{3/2} \tag{16}$$

in which

$$\sim = \sim_o (1+u)^{3/2} \tag{17}$$

The total head  $H_d$  is expressed as:

$$H_d = h_d + \frac{Q^2}{2gA^2} \tag{18}$$

With  $A = B(h_d + P)$ , equation (18) becomes:

$$H_d = h_d + \frac{Q^2}{2gB^2(h_d + P)^2} \tag{19}$$

According to equations (1), (2) and (19), one can write:

$$H_d^* = h_d^* + \frac{\mathbb{E}^2}{2h_d^{*2}} \quad (20)$$

where  $H_d^* = H_d / h_c$ . Comparing equations (4) and (20) yields:

$$u = \frac{\mathbb{E}^2}{2h_d^{*3}} \quad (21)$$

From equations (8), (9) and (21), one may deduce that the kinetic factor  $u$  depends solely on the non-dimensional parameter  $\mathbb{E} (s, P^*)$ . Inserting equation (21) into equation (17) leads to:

$$\sim = \sim_o \left( 1 + \frac{\mathbb{E}^2}{2h_d^{*3}} \right)^{3/2} \quad (22)$$

Combining equations (11) and (22) yields:

$$\sim = \sim_o \left( 1 + \sim_o^2 \mathbb{E}^2 \right)^{3/2} \quad (23)$$

Equation (23) expresses the discharge coefficient of the considered device taking into account the effect of the approach velocity of the flow. According to equation (16), the discharge  $Q$  is governed by what follows:

$$Q = \sim_o \left( 1 + \sim_o^2 \mathbb{E}^2 \right)^{3/2} b \sqrt{2g} h_d^{3/2} \quad (24)$$

Taking into account equation (12), equation (24) becomes:

$$Q = \frac{1}{4} \cos^{-3/2} (r/3) \left[ 1 + \frac{\mathbb{E}^2}{16} \cos^{-3} (r/3) \right]^{3/2} b \sqrt{2g} h_d^{3/2} \quad (25)$$

#### 4.5. Example 2

Let the data of the example 1 and compute the discharge  $Q$  taking into account the effect of the approach velocity.

According to equation (25), the requested discharge  $Q$  is:

$$\begin{aligned} Q &= \frac{1}{4} \cos^{-3/2} (r/3) \left[ 1 + \frac{\mathbb{E}^2}{16} \cos^{-3} (r/3) \right]^{3/2} b \sqrt{2g} h_d^{3/2} \\ &= \frac{1}{4} \times \cos^{-3/2} (1.87548898/3) \times \left[ 1 + \frac{0.3^2}{16} \times \cos^{-3} (1.87548898/3) \right]^{3/2} \times 0.5 \times \sqrt{2 \times 9.81} \times 0.6^{3/2} \\ &= 0.358 m^3 s^{-1} \end{aligned}$$

It thus appears that when the approach velocity is neglected, the relative error in the calculation of the discharge  $Q$  is:

$$\Delta Q / Q = 100 \times \frac{0.358 - 0.3524}{0.358} \cong 1.56\%$$

## 5. Experimental Verification

In this part of the study, the experimental protocol used to verify the proposed theoretical relationships is presented. The studied device has been subjected to an intense experimental programme, for different values of the contraction rate  $S$  and the relative weir height  $P^*$ .

### 5.1. Characteristics of the tested devices

To study the effect of the contraction rate and the relative weir height, several devices have been designed and tested. These were constructed in transparent Plexiglas to permit visualization of the flow. All tested devices were inserted in a rectangular channel from which the discharge  $Q$  is to be evaluated. Thirteen devices with a height crest were tested and subjected to wide ranges of the discharge  $Q$  and the head  $h_d$  over the crest. Experimental tests have yielded 260 measures of the head-discharge law. The experiment also involved eight devices without height crest ( $P = 0$ ) and yielded more than 157 measures of the head-discharge law. Tables 1 and 2 include the geometric characteristics of the tested devices and the hydraulic characteristics of the resulted flow.

Table. 1 : Geometric characteristics of the tested devices with a height crest  
( $P \neq 0$ )

Device	Contraction rate $s$	Weir height $P$ (cm)	Number of measures	Discharge ranges	Head ranges
1	0.501	10	20	$2.08 \text{ l/s} \leq Q \leq 26.60 \text{ l/s}$	$4.63 \text{ cm} \leq h_d \leq 23.97 \text{ cm}$
2	0.501	8	20	$1.45 \text{ l/s} \leq Q \leq 23.47 \text{ l/s}$	$3.66 \text{ cm} \leq h_d \leq 21.99 \text{ cm}$
3	0.501	6	20	$2.00 \text{ l/s} \leq Q \leq 23.17 \text{ l/s}$	$4.41 \text{ cm} \leq h_d \leq 21.62 \text{ cm}$
4	0.45	8	20	$1.63 \text{ l/s} \leq Q \leq 24.67 \text{ l/s}$	$4.26 \text{ cm} \leq h_d \leq 24.70 \text{ cm}$
5	0.45	6	20	$2.00 \text{ l/s} \leq Q \leq 21.52 \text{ l/s}$	$4.80 \text{ cm} \leq h_d \leq 22.32 \text{ cm}$
6	0.399	10	20	$2.37 \text{ l/s} \leq Q \leq 22.13 \text{ l/s}$	$5.90 \text{ cm} \leq h_d \leq 25.33 \text{ cm}$
7	0.399	8	20	$1.67 \text{ l/s} \leq Q \leq 24.92 \text{ l/s}$	$4.64 \text{ cm} \leq h_d \leq 27.02 \text{ cm}$
8	0.399	6	20	$1.88 \text{ l/s} \leq Q \leq 19.73 \text{ l/s}$	$5.03 \text{ cm} \leq h_d \leq 23.07 \text{ cm}$
9	0.348	8	20	$2.02 \text{ l/s} \leq Q \leq 18.82 \text{ l/s}$	$5.83 \text{ cm} \leq h_d \leq 24.83 \text{ cm}$
10	0.348	6	20	$2.90 \text{ l/s} \leq Q \leq 23.50 \text{ l/s}$	$7.30 \text{ cm} \leq h_d \leq 28.74 \text{ cm}$
11	0.3	10	20	$2.68 \text{ l/s} \leq Q \leq 18.30 \text{ l/s}$	$7.76 \text{ cm} \leq h_d \leq 27.20 \text{ cm}$
12	0.3	8	20	$2.77 \text{ l/s} \leq Q \leq 18.22 \text{ l/s}$	$7.89 \text{ cm} \leq h_d \leq 27.20 \text{ cm}$
13	0.3	6	20	$1.40 \text{ l/s} \leq Q \leq 17.77 \text{ l/s}$	$5.06 \text{ cm} \leq h_d \leq 26.53 \text{ cm}$

Table. 2 : Geometric characteristics of the tested devices without height crest ( $P = 0$ )

Device	Contraction rate S	Number of measures	Discharge ranges	Head ranges
1	0.15	19	2.38 l/s $\frac{1}{2}$ $Q$ $\frac{1}{2}$ 13.18 l/s	9.94 cm $\frac{1}{2}$ $h_d$ $\frac{1}{2}$ 31.49 cm
2	0.181	20	2.76 l/s $\frac{1}{2}$ $Q$ $\frac{1}{2}$ 17.11 l/s	10.04 cm $\frac{1}{2}$ $h_d$ $\frac{1}{2}$ 33.02 cm
3	0.201	19	2.15 l/s $\frac{1}{2}$ $Q$ $\frac{1}{2}$ 18.11 l/s	7.66 cm $\frac{1}{2}$ $h_d$ $\frac{1}{2}$ 32.02 cm
4	0.253	19	1.61 l/s $\frac{1}{2}$ $Q$ $\frac{1}{2}$ 18.18 l/s	5.58 cm $\frac{1}{2}$ $h_d$ $\frac{1}{2}$ 27.46 cm
5	0.30	20	2.95 l/s $\frac{1}{2}$ $Q$ $\frac{1}{2}$ 24.77 l/s	7.28 cm $\frac{1}{2}$ $h_d$ $\frac{1}{2}$ 29.51 cm
6	0.35	20	2.00 l/s $\frac{1}{2}$ $Q$ $\frac{1}{2}$ 24.01 l/s	5.10 cm $\frac{1}{2}$ $h_d$ $\frac{1}{2}$ 26.31 cm
7	0.40	20	1.81 l/s $\frac{1}{2}$ $Q$ $\frac{1}{2}$ 25.11 l/s	4.34 cm $\frac{1}{2}$ $h_d$ $\frac{1}{2}$ 24.60 cm
8	0.45	20	2.33 l/s $\frac{1}{2}$ $Q$ $\frac{1}{2}$ 28.18 l/s	4.72 cm $\frac{1}{2}$ $h_d$ $\frac{1}{2}$ 24.37 cm

## 5.2. Test sequence

Each of the devices given in the tables 1 and 2 was tested in a rectangular channel of width equal to  $B=0.293m$ . From the control valve of the closed circuit of the test bench, a discharge  $Q$  was selected. The resulting flow is clearly shown in figure 3.



Fig.3. Upstream view of both the tested device and the resulting flow

The head  $h_d$  over the device crest was measured by reading a gauge of double accuracy. This is represented by figure 4.



Fig.4. Head gauge of double accuracy

Each device has been tested under a wide range of discharge  $Q$  (Tables 1 and 2) whose value has been carefully determined using an ultrasonic flow meter. The known values of the width device  $b$ , the crest height  $P$ , the width  $B$  of the rectangular channel and the head  $h_d$  were used to calculate the following parameters:

- Contraction rate  $S = b / B$
- Relative weir height  $P^* = P / h_d$ , for each experimental discharge
- The non-dimensional parameter  $\mathbb{E} = S / (1 + P^*)$
- The discharge coefficient  $\tilde{c}_o$  for a neglected approach velocity such as  $\tilde{c}_o = Q / (b\sqrt{2g}h_d^{3/2})$ , for each experimental discharge.

### 5.3. Discharge coefficient for a significant approach velocity

From the known values of the experimental parameters  $\tilde{c}_o$  and  $\mathbb{E}$ , the discharge coefficient  $\tilde{c}$  for a significant approach velocity was calculated according to equation (23). All the obtained experimental values of the discharge coefficient  $\tilde{c}$  are shown in figure 5. In the same figure the curves corresponding to  $\tilde{c}_{th}$  and  $0.99\tilde{c}_{th}$  are represented, where  $\tilde{c}_{th}$  is the theoretical discharge coefficient computed from equation (23) for the values of  $\mathbb{E}$  arbitrarily chosen. In addition, discharge coefficients  $\tilde{c}(P = 0)$  are represented in figure 5 by the open signs.

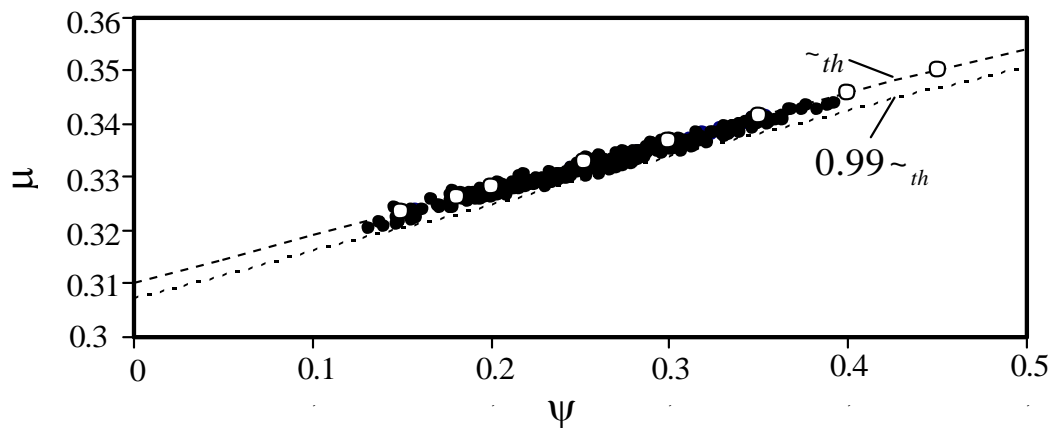


Fig.5. Discharge coefficient  $\tilde{C}_d(\Xi)$  for a significant approach velocity

(●) Experimental points for  $P \neq 0$ , (○) Experimental points for  $P = 0$ .

(- - -) Theoretical curves plotted according to equation (23)

In view of figure 5, it appears that all observation data are located between the theoretical curves  $\tilde{C}_d^{th}$  and  $0.99\tilde{C}_d^{th}$ . This allows the conclusion that the theoretical relation (23) can be used as it is quiet accurate. This relationship is applicable to all devices of the same tested type including those without crest height.

## 6. Conclusions

The study of semi-modular rectangular cross section flow meter with a lateral contraction was presented. The main objective was to determine the expressions of both discharge coefficient of the device and discharge, taking into account the effect of the approach velocity. A theoretical approach was proposed to model the discharge coefficient in the general case of a device with a crest height. This theoretical approach was based on the momentum equation applied between two selected cross sections of the flow. The obtained relationship was presented in dimensionless terms [Eq. (7)], after defining the parameter  $\Xi$  corresponding to the contraction rate of inflow cross section. This parameter includes both the effect of lateral contraction rate of the device and the relative height of the weir. Equation (7) showed that the relative head over the sill was related to the parameter  $\Xi$  only. By the use of trigonometric functions, it was possible to determine the explicit relationship  $h_d^*(\Xi)$  [Eq. (8)]. In practice, the known parameter being  $\Xi$ , equation (8) allows then to compute on one hand the relative head over the sill and the discharge coefficient  $\tilde{C}_d$  for a disregarded approach velocity on the other hand according to equation (11). Thus, applying equation (13) discharge  $Q$  is worked out. If the effect of approach velocity must be taken into account, discharge coefficient can be explicitly evaluated using equation (23). The discharge  $Q$  is computed according to the explicit equation (25). The practical application of the obtained theoretical relationships was illustrated through some numerical examples.

The studied device was then subjected to an intense experimental programme. It has been tested in several geometric dimensions. The aim was to verify the validity of the proposed theoretical relationships, especially the relationship (23) which expresses the theoretical discharge coefficient. It has been observed (Fig. 5) that the experimental observations lie between the curves  $\sim_{th}$  and  $0.99\sim_{th}$ , that substantiate the validity of equation (23).

It should finally be noted that the configuration corresponding to  $P = 0$  is simple and convenient as it is reduced to a lateral contraction of the device whose realization is easy to implement. For this configuration, Figure 5 shows that the experimental points align perfectly with the theoretical curve of the discharge coefficient, implying that equation (25) can be applied with remarkable accuracy.

### Nomenclature

$A$	Section area ( $m^2$ )
$b$	Weir width (m)
$B$	Rectangular channel width (m)
$F$	Pressure force (N)
$g$	Acceleration due to gravity ( $ms^{-2}$ )
$H_d$	Total head over a weir (m)
$h_0$	Channel height
$h_m$	Minimum depth
$h_d$	Head over a weir (m)
$h_c$	Critical depth (m)
$h_d^*$	Relative head (-)
$L$	Weir length (m)
$P$	Weir height (m)
$Q$	Discharge ( $m^3s^{-1}$ )
$V$	Mean velocity ( $ms^{-1}$ )
$X$	Longitudinal coordinate
$s$	Width ratio (-)
$\xi$	Ratio of the contracted upstream flow
$\Delta H$	Head loss (m)
$u$	Kinetic factor (-)
$\sim$	Discharge coefficient (-)
$\dots$	Water density ( $kgm^{-3}$ )

## References

- [1] Bos M.G. Discharge measurement structures, *Laboratorium voor hydraulica aan Afvoerhydrologie* 1976; Landbouwhogeschool, Wageningen, The Netherlands, Rapport 4, May.
- [2] Bos M.G. Discharge measurement structure, 3<sup>rd</sup> Ed., Publication 20, *Int. Institute for Land Reclamation and Improvement* 1989; Wageningen, Netherlands.
- [3] De Coursey D.E., Blanchard B.J. Flow analysis over large triangular weir, *Proc. ASCE, J. Hyd. Div.* 1970; 96 (HY7): 1435-1454.
- [4] Rao N.S.L. Theory of weir, *Advances in hydrodynamics, Ed. Ven Te Chow* 1963; N.Y.
- [5] Bazin H. Expériences nouvelles sur l'écoulement en déversoir, *Ed. Dunod, Paris* 1898.
- [6] Kindsvater C.E, Carter R.W. Discharge characteristics of rectangular thin-plate weirs, *Proc. ASCE, J. Hyd. Div.* 1957; 83 (HY6) : 1453/1-6.
- [7] SIA. Contribution à l'étude des méthodes de jaugeage, Bull. 18, *Schw. Bureau Wasserforschung* 1926; Bern.
- [8] Achour B. Débitmètre à ressaut en canal de section droite triangulaire sans seuil, *J. Hydr. Research* 1989; 27(2): 205-214.
- [9] Hager W.H. (1985). Modified Venturi channel, *Proc. ASCE, J. Irrigation and Drainage Engineering* 1985; 111(IR1): 19-35.
- [10] Bouslah S. Theoretical and experimental analysis of broad-crested triangular weir, Magister Thesis, department of hydraulics 2006; University of Biskra, Algeria.
- [11] Achour B., Bouziane M.T., Nebbar K. Broad-crested triangular flowmeter in rectangular channel, *Larhyss Journal* 2003; n°03: 7-43.
- [12] Kechida S. Theoretical and experimental analysis of a flow over a wide rectangular sill, Magister thesis 2006; Department of hydraulics, University of Biskra, Algeria.
- [13] Hachemi Rachedi L. Flow analysis trough a lateral contraction, Magister thesis 2006; Department of hydraulics, University of Biskra, Algeria.
- [14] Hager W.H. Discharge measurement structures, *Communication 1* 1986 ; Département de Génie-Civil, Ecole Polytechnique Fédérale de Lausanne, Suisse.
- [15] Brandes D., Barlow W.T. New Method for Modeling Thin-Walled Orifice Flow Under partially Submerged Conditions, *J. Irrig. Drain. Eng.* 2012; 138(10): 924-928.
- [16] Vatankhah A.R., Bijankhan M. Discussion of New Method for Modeling Thin-Walled Orifice Flow Under partially Submerged Conditions, *J. Irrig. Drain. Eng.* 2013; 139: 789-793.